Vapor-liquid equilibrium of water with the MB-pol many-body potential

Maria Carolina Muniz,[1, a)] Thomas E. Gartner III,[2, a)] Marc Riera,[3] Christopher Knight,[4] Shuwen Yue,[1] Francesco Paesani,[3, 5, 6, b)] and Athanassios Z. Panagiotopoulos[1, c)]

[1)] *Department of Chemical and Biological Engineering, Princeton University, Princeton, New Jersey 08544, USA*

[2)] *Department of Chemistry, Princeton University, Princeton, New Jersey 08544, USA*

[3)] *Department of Chemistry and Biochemistry, University of California, San Diego, La Jolla, California 92093, USA*

[4)] *Computational Science Division, Argonne National Laboratory, Argonne, Illinois 60439, USA*

[5)] *Materials Science and Engineering, University of California San Diego, La Jolla, California 92093, USA*

[6)] *San Diego Supercomputer Center, University of California San Diego, La Jolla, California 92093, USA*

(Dated: 15 March 2021)

Among the many existing molecular models of water, the MB-pol many-body potential has emerged as a remarkably accurate model, capable of reproducing thermodynamic, structural, and dynamic properties across water's solid, liquid, and vapor phases. In this work, we assessed the performance of MB-pol with respect to an important set of properties related to vapor-liquid coexistence and interfacial behavior. Through direct coexistence classical molecular dynamics simulations at temperatures 400 K $< T <$ 600 K, we calculated properties such as equilibrium coexistence densities, vapor-liquid interfacial tension, vapor pressure, and enthalpy of vaporization, and compared the MB-pol results to experimental data. We also compared rigid vs. fully flexible variants of the MB-pol model and evaluated system size effects for the properties studied. We found that the MB-pol model predictions are in good agreement with experimental data, even for temperatures approaching the vapor-liquid critical point; this agreement was largely insensitive to system size or the rigid vs. flexible treatment of the intramolecular degrees of freedom. These results attest to the chemical accuracy of MB-pol and its high degree of transferability, thus enabling MB-pol's application across a large swath of water's phase diagram.

I. INTRODUCTION

Water has been the focus of many computational studies[1–4], given its biological and industrial importance and its often intriguing behavior. However, developing a model that accurately describes the thermophysical properties of water from gas to the condensed phases is a challenging task due to the complexity of water's intermolecular interactions. As a representative example, one important set of phenomena that has been the focus of many computational studies is water's vapor-liquid equilibrium (VLE)[5–10]. Accurately predicting water's VLE behavior is important due to the key role it plays in several industrial applications, such as distillation and the production of electricity via steam turbines. The early stages of the liquid-vapor phase transformation, marked by bubbles appearing in liquid water in a process termed cavitation, is also a concern to engineering applications, since it often results in damages to pumps and turbines.

In an ideal case, correlated quantum chemistry methods would be used to sample water's potential energy surface (PES) from first principles, but the computational expense of such techniques make comprehensive predictions of water's bulk thermodynamic properties and phase behavior largely out of reach with current computational resources. Due to the high computational cost involved in *ab initio* molecular dynamics (MD) simulations, and despite broad interest and the potential utility of predictive simulations of water VLE, relatively few 'first principles' investigations of water VLE have been reported to date[10–13].

As an alternative to costly quantum chemistry methods, empirical force fields have been developed to study water-related phenomena via classical molecular simulations[14–27]. To date, the most-used empirical representations of water consist of fixed-charge, rigid, non-polarizable models built on pairwise interaction potentials, such as SPC/E[16], TIP3P[17] and TIP4P/2005[19]. Due to their simplicity and computational efficiency, these models allow for simulations of significantly larger systems and/or greater timescales than *ab initio* approaches and are often able to reproduce many important properties of liquid water[3]. However, when it comes to reproducing simultaneously vapor phase and VLE properties, such as vapor pressures and densities, surface tension, and critical properties, many pairwise rigid and/or non-polarizable models fall short[3,8,28], often due to their inability to represent polarization and/or many-body ef-

a)These authors contributed equally to this work.

b)Electronic mail: fpaesani@ucsd.edu

c)Electronic mail: azp@princeton.edu

fects.

With that in mind, more advanced empirical models have been developed, such as E3B[14,15], which includes a three-body term, and polarizable models, such as AMOEBA[24–27], the Baranyai–Kiss models (BK3)[23] and the Hydrogen-Bonding Polarizable (HBP) model[22]. The inclusion of polarization results in better accuracy when computing properties related to VLE and the gas phase, such as virial coefficients, vapor pressures, and critical properties[22–27]. However, empirical models parameterized to reproduce certain experimental results may still lack in transferability, which could limit their use to predict water's properties across the phase diagram. Furthermore, studies suggest that including many-body polarization effects might be a way of improving transferability in empirical models, specially for calculating properties of VLE related phenomena, such as liquid droplet nucleation from a supersaturated vapor phase[29].

One notable advanced many-body model for water is the MB-pol potential[30–32]. MB-pol was constructed to reproduce interaction energies based on high-level coupled-cluster theory calculations–often referred to as the 'gold standard' among quantum chemistry methods– and explicitly accounts for many-body effects through a rigorous many-body expansion of the intra- and intermolecular energies. MB-pol was shown to have excellent agreement with the coupled cluster reference calculations in terms of interaction energies, and accurately reproduces many structural and thermodynamic properties of water, from gas to the condensed phases[2,33–35]. However, the VLE behavior of MB-pol has not yet been comprehensively explored, particularly at elevated temperatures, partially due to the increased computational cost of MB-pol relative to other advanced water models[33].

In this work, we used a new implementation of MB-pol in the MBX[36] library interfaced with the LAMMPS[37] molecular simulation software. The MBX library serves as an engine to compute potential energies, forces, and virials according to the many-body MB-pol model, and can be in principle interfaced with any desired molecular simulation code (e.g., LAMMPS[37], i-PI[38], OpenMM[39]). Using direct-coexistence MD simulations[7,9,40–42] in this MBX/LAMMPS framework, we assessed MB-pol's ability to reproduce properties such as equilibrium coexistence densities, interfacial tension, and enthalpy of vaporization, for a broad range of elevated temperatures 400 K $< T <$ 600 K. The new coupling of MBX with LAMMPS allowed us to leverage the highly parallelizable nature of the LAMMPS codebase to access the system sizes and time scales necessary to produce converged interfacial simulations.

The article is organized as follows. In section II, we briefly discuss the construction of the MB-pol water model and our new LAMMPS-based implementation, as well as simulation and analysis details. In section III we present a discussion around the results obtained and the overall performance of the potential in predicting water's VLE. Finally, in section IV we provide a summary of the work and mention possible future investigations.

II. METHODS

A. MB-pol model details and LAMMPS implementation

MB-pol is a many-body potential energy function (PEF) entirely derived from *ab initio* reference data, and takes advantage of the fast convergence of the many-body expansion (MBE)[43] of the energy of a system. MBE states that the total energy of a system can be exactly decomposed as

$$E_N(1,\ldots,N) = \sum_{i=1}^{N} V^{1B}(i) + \sum_{i<j}^{N} V^{2B}(i,j)$$
$$+ \sum_{i<j<k}^{N} V^{3B}(i,j,k) \qquad (1)$$
$$+ \cdots + V^{NB}(1,\ldots,N),$$

where $V^{nB}(i,...,m)$ defines the n-body energy involving n monomers $i,...,m$ (in this case each 'monomer' is one water molecule). MB-pol has an explicit one-body term described by the PES developed by Partridge and Schwenke,[44] and the long range interactions are modeled with two-body dispersion damped with the Tang-Toennies damping function (V^{2B}_{disp})[45] and a slightly modified Thole-type model as introduced in the TTM4-F model[46] for the electrostatic interactions, which include two-body permanent electrostatics (V^{2B}_{perm}) and many-body classical polarization (V^{nB}_{ind}). The two- and three-body terms are supplemented with a correction through permutationally invariant polynomials,[47] V^{2B}_{poly} and V^{3B}_{poly}, respectively, fitted to reproduce two- and three-body reference energies calculated with coupled-cluster with single, double, and perturbative triple excitations (CCSD(T)). These polynomial functions correct for the deficiencies of the classical expressions at short range due to quantum effects such as charge penetration, charge transfer, and Pauli repulsion. Further details of the MB-pol PEF can be found the the MB-pol paper series.[30,31]

In the standard MB-pol model, intramolecular degrees of freedom are unconstrained, necessitating a small timestep size in MD simulations to accurately capture the motion of the hydrogen atoms. In order to access longer simulation time scales, we also tested a rigid variant of the MB-pol model, in which we constrained the H-O bond length and H-O-H angle to the average values obtained from the flexible MB-pol simulations: 0.969 Å and 104.7°, respectively. This rigid variant of the model allowed us to increase the timestep by a factor of 10 as detailed below.

The MBX library implementing the MB-pol model[36] is tightly coupled with the LAMMPS code[37] with the objective of targeting large-scale molecular simulations on

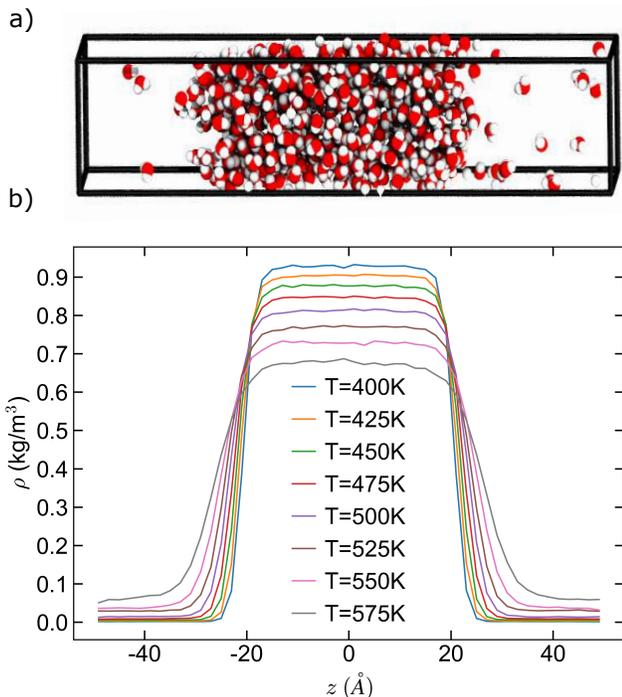high-performance computing resources.

a)

b)

FIG. 1. (a.) Representative snapshot showing the direct coexistence geometry with 512 molecules at $T = 500$ K. (b.) Average density profiles obtained from the direct coexistence MD simulations for the MB-pol rigid version with 512 molecules. Colors denote different temperatures as noted.

direct coexistence geometry at $T = 500$ K, as well as averaged density profiles for the 512 molecule rigid MB-pol system. As expected, the system maintained a clear separation between liquid and vapor regions, with the vapor density and interfacial width increasing as temperature increased. For the 512 molecule system size, we explored state points ranging from $T = 400$ K to $T = 575$ K in order to maintain the reliability of the coexistence density calculations. $T < 400$ K resulted in too few molecules in the vapor phase for a reliable density estimate, while $T > 575$ K resulted in poorly-defined liquid and vapor regions. For the larger 1024 molecule system, we added $T = 600$ K, as the vapor-liquid interface was more stable close to the critical point in the larger system.

Figure 2 shows that for all three systems considered, MB-pol vapor and liquid densities were in excellent agreement with experimental results. While the overall agreement in VLE densities was quite good, the phase envelope from MB-pol was predicted to be slightly narrower than the experiments for $T > 500$ K. The liquid densities of the rigid MB-pol model were slightly lower than the fully flexible version, but the predicted vapor phase densities were within estimated uncertainties in all three cases. There were minimal differences in the coexistence densities from the rigid MB-pol model at different system size.

From the coexistence densities we also estimated the critical parameters for each system. For the flexible MB-pol model we found $T_c = 639\pm14$ K and $\rho_c = 0.34\pm0.03$ g/cm^3, for rigid MB-pol at 512 molecules $T_c = 640\pm6$ K and $\rho_c = 0.33\pm0.01$ g/cm^3, and for rigid MB-pol 1024 molecules $T_c = 635\pm9$ K and $\rho_c =0.33\pm0.02$ g/cm^3. These estimated values for the critical parameters were close to the experimental values ($T_c = 647.1$ K and $\rho_c = 0.322$ g/cm^3)[50], and all within uncertainty of one another. The predicted T_c for the 1024 molecule system size was slightly lower than the smaller systems, likely due to the inclusion of one more point ($T = 600$ K) in the critical point calculation. Relative to experiments, the MB-pol model slightly underestimates the critical temperature and overestimates the critical density. Finite size effects may play a role in the predicted coexistence densities and estimated critical parameters obtained herein, as the limited system dimensions limit the wavelength of density fluctuations that can develop (as well as limiting development of capillary waves along the liquid-vapor interface). However, the impact of the finite system size is nontrivial in an interfacial system[51,52], and it is difficult to say *a priori* whether in the infinite system our estimated critical parameters would increase or decrease. As such, a rigorous investigation of system size effects–including an extrapolation to the thermodynamic limit–is necessary to fully evaluate these predictions, which is currently too computationally expensive with this model. In future work (as the highly-parallel LAMMPS MB-pol implementation continues to be optimized), we plan to return to the issue of system size effects for a rigorous critical point estimate.

A key advantage of the direct coexistence approach to VLE calculations is that, in addition to vapor and liquid coexistence densities, one can obtain important characterizations of the interfacial properties. In particular, analysis of the pressure tensor from the simulation results provides access to the vapor-liquid surface tension, γ (related to the stability of the interface), as well as the saturation vapor pressure, P_{vap}, which we plot in Figure 3. For the three systems studied, surface tension results were in excellent agreement with experimental results across the temperature range considered, and did not differ as a function of bond/angle flexibility or system size. Similarly, the P_{vap} agreed closely with the experimental results for $T < 500$ K and slightly over-predicted the experimental value at high temperatures, which corresponds with the slightly overpredicted vapor density as the system approaches the critical temperature (Figure 2). These quantities provide additional illustrations of the ability of the MB-pol model to accurately reproduce VLE and interfacial properties of water.

Finally, we also estimated thermodynamic quantities such as the enthalpy of vaporization, ΔH_{vap}, as a function of temperature (Figure 4). Similar to the saturation vapor pressure, ΔH_{vap} values had no significant differences among the model variants, and agreed closely with experimental data for $T < 500$ K. Uncertainties were somewhat higher with the flexible MB-pol model,

a)

b)
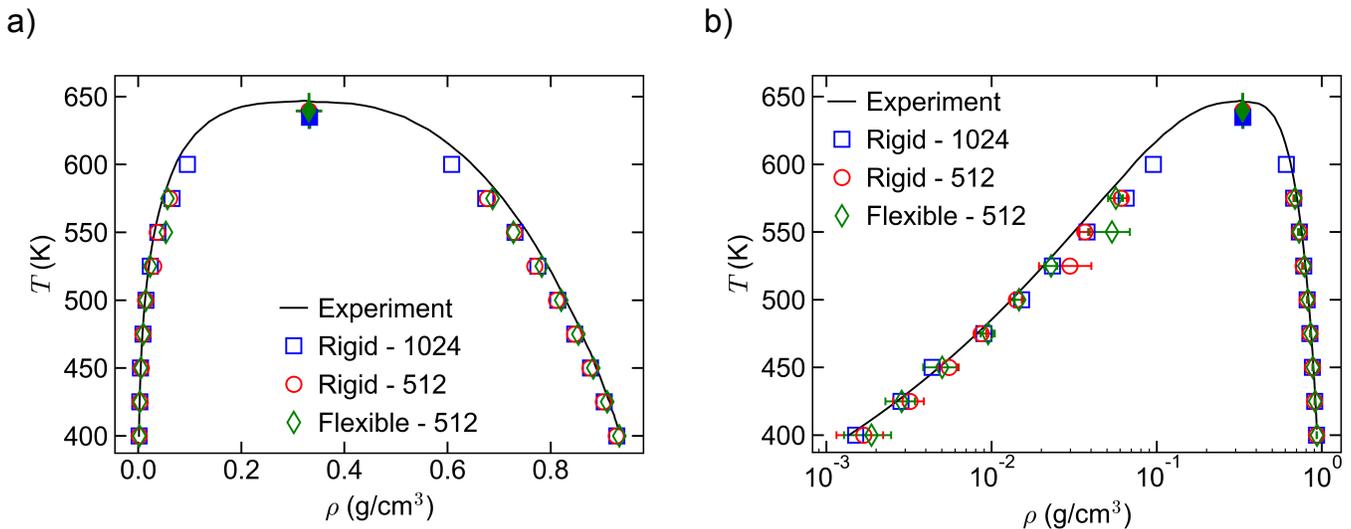
FIG. 2. (a.) Vapor-liquid coexistence curves (vapor and liquid mass density ρ as a function of temperature T) for the three different cases studied: MB-Pol rigid model with 512 molecules (red circles), MB-Pol rigid model with 1024 molecules (blue squares), MB-Pol flexible model with 512 molecules (green diamonds).(b.) Same data as (a.) presented on a log-scale in ρ to display the vapor phase densities. In both panels, coexistence densities are represented as open symbols, estimated critical points are represented as filled symbols, and experimental data[50] are shown as solid lines. Statistical uncertainties are at the 95% confidence level and are shown only when larger than the symbol size. Tabulated simulation densities and uncertainties can be found in Supporting Information.

a)

b)
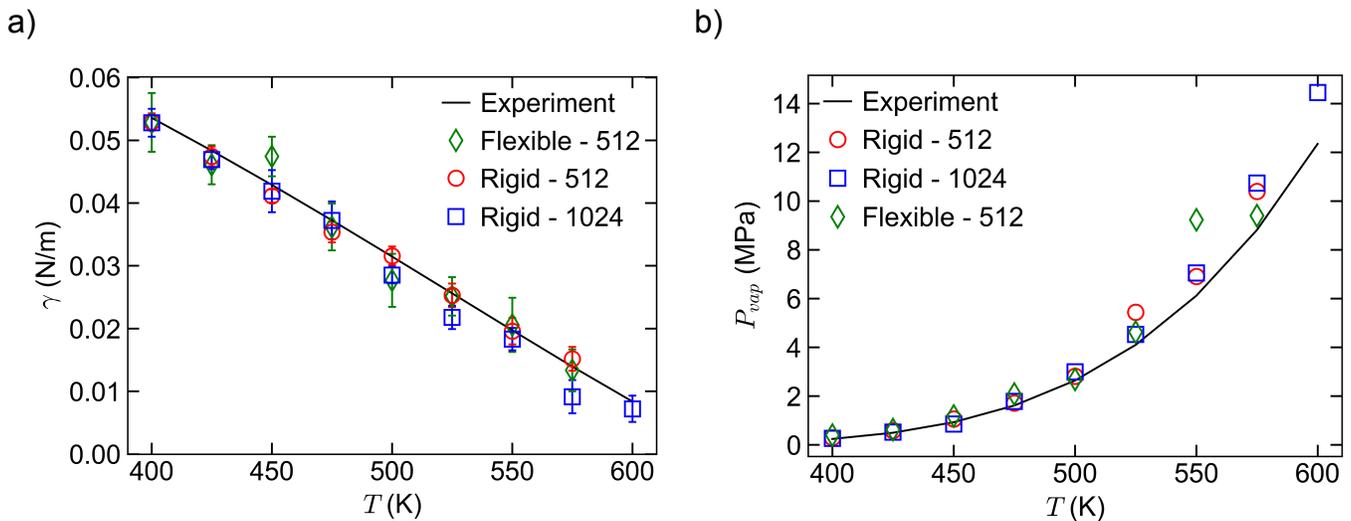
FIG. 3. (a.) Surface tension, γ, and (b.) saturation vapor pressure, P_{vap}, for rigid MB-Pol with 512 molecules (red circles), rigid MB-Pol with 1024 molecules (blue squares), flexible MB-Pol with 512 molecules (green diamonds) as a function of temperature. Experimental data[50] are shown as solid lines. Statistical uncertainties are at the 95% confidence level and are shown only when larger than the symbol size. Tabulated averages and uncertainties can be found in Supporting Information.

likely due to the shorter accessible simulation timescales. At high temperature, MB-pol slightly underpredicted ΔH_{vap}, again in line with the narrower phase envelope in that regime of temperatures. We note that in Ref. 33, which explored water's thermophysical properties for $T < 368$ K, MB-pol was found to overpredict ΔH_{vap}, with the agreement between simulation and experiment improving as T increased. Combined with our results,

this trend indicates a crossover between the MB-pol and experimental ΔH_{vap} somewhere in the vicinity of $T = 400$ K. Notwithstanding, we emphasize the overall close agreement between simulation and experimental ΔH_{vap} across a wide range of temperatures.

Taken together, these results show the utility of MB-pol as an accurate predictive model of water's vapor-liquid phase behavior across a wide range of elevated

temperatures. MB-pol predicts liquid and vapor coexistence densities, interfacial energetics, and thermodynamic phase change data in close agreement with experimental results. Such agreement is notable because MB-pol was parameterized to reproduce the energetics of isolated 2-body and 3-body clusters, and does not include condensed phases or interfacial configurations in the reference data set.[30–32] MB-pol's accuracy in reproducing the properties of liquid water has been well established[33], herein we show that the model's construction is also sufficient for high quality descriptions of the vapor-liquid interface and phase behavior. Another interesting result is the relatively minor differences in the properties of the rigid and flexible versions of MB-pol, allowing one to access significantly larger simulation timescales (while maintaining a similar degree of predictive accuracy) for systems where intramolecular degrees of freedom are unimportant. Unlike fixed-charge models, which tend to show differences in the properties of their rigid and flexible variants[53,54], the electrostatic charges in MB-pol are free to instantaneously respond to the environment and to the monomer geometry, thus resulting in minimal differences upon fixing the intramolecular degrees of freedom for the properties explored herein. Lastly, system size effects appear to be minimal for the interfacial geometries explored in this work, though we plan to more thoroughly explore system size effects as our LAMMPS implementation continues to be optimized for computational efficiency.

FIG. 4. Enthalpy of vaporization, ΔH_{vap}, for rigid MB-Pol with 512 molecules (red circles), rigid MB-Pol with 1024 molecules (blue squares), flexible MB-Pol with 512 molecules (green diamonds) as a function of temperature. Experimental data[50] are shown as solid lines. Statistical uncertainties are at the 95% confidence level and are shown only when larger than the symbol size. Tabulated averages and uncertainties can be found in Supporting Information.
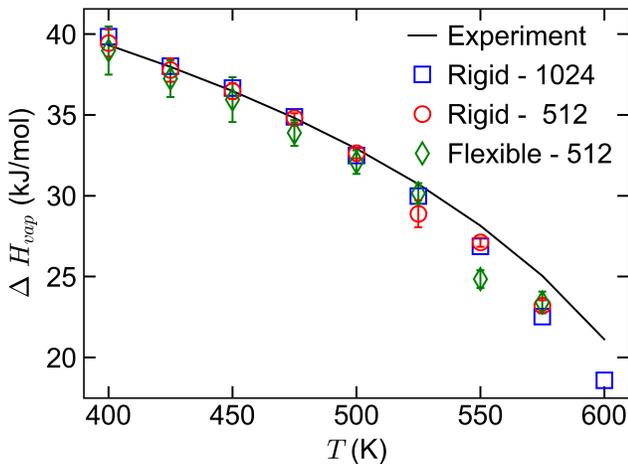
IV. CONCLUSION

In this work, we investigated the vapor-liquid equilibrium properties of water with the many-body MB-pol potential. Through direct coexistence classical MD simulations, we assessed the accuracy of MB-pol in reproducing water's properties, including coexistence densities, surface tension, vapor pressure, and enthalpy of vaporization. We also evaluated system size effects and the impact of rigid vs. flexible model variants for all properties explored. A new implementation of MB-pol as a library in LAMMPS allowed us to access system sizes and simulation length scales never before achieved with the MB-pol model, and produce converged thermodynamic properties in the direct coexistence geometry.

The MB-pol results were in excellent agreement with experimental data, providing additional evidence of MB-pol's ability to accurately reproduce water's thermophysical properties across the phase diagram. Specifically in this paper, we show how MB-pol's transferability can be extended to study a heterogeneous system, water's VLE, which has important industrial applications. Furthermore, the rigid variant of the model was nearly identical to the flexible version, allowing access to even longer length and time scales. In future work, we plan to rigorously explore system size effects to allow extrapolation to the thermodynamic limit. Lastly, a similar approach could be used to investigate the structure of interfacial water from first principles, providing a predictive analysis of hydrogen bonding and water's molecular arrangement at the vapor-liquid interface for elevated temperatures.

V. SUPPLEMENTARY MATERIALS

The supplementary materials include tabulated liquid and vapor coexistence densities, surface tension values, vapor pressures, and enthalpy of vaporization, as well as the statistical uncertainties for these quantities.

VI. ACKNOWLEDGMENTS

VII. AIP PUBLISHING DATA SHARING POLICY

The data that support the findings of this study are available from the corresponding authors upon reasonable request.

VIII. REFERENCES

[1] P. Gallo, K. Amann-Winkel, C. A. Angell, M. A. Anisimov, F. Caupin, C. Chakravarty, E. Lascaris, T. Loerting, A. Z. Panagiotopoulos, J. Russo, J. A. Sellberg, H. E. Stanley, H. Tanaka, C. Vega, L. Xu, and L. G. M. Pettersson, "Water: A tale of two liquids," Chemical Reviews 116, 7463–7500 (2016), pMID: 27380438.

[2] G. A. Cisneros, K. T. Wikfeldt, L. Ojamäe, J. Lu, Y. Xu, H. Torabifard, A. P. Bartók, G. Csányi, V. Molinero, and F. Paesani, "Modeling Molecular Interactions in Water: From Pairwise to Many-Body Potential Energy Functions," Chemical Reviews 116, 7501–7528 (2016).

[3] C. Vega and J. L. F. Abascal, "Simulating water with rigid non-polarizable models: a general perspective," Physical Chemistry Chemical Physics 13, 19663–19688 (2011).

[4] M. J. Gillan, D. Alfè, and A. Michaelides, "Perspective: How good is DFT for water?" The Journal of Chemical Physics 144, 130901 (2016), 1603.01990.

[5] B. Chen, J. Xing, and J. I. Siepmann, "Development of polarizable water force fields for phase equilibrium calculations," The Journal of Physical Chemistry B 104, 2391–2401 (2000).

[6] F. Moučka and I. Nezbeda, "Gibbs ensemble simulation on polarizable models: Vapor-liquid equilibrium in Baranyai-Kiss models of water," Fluid Phase Equilibria 360, 472–476 (2013).

[7] A. E. Ismail, G. S. Grest, and M. J. Stevens, "Capillary waves at the liquid-vapor interface and the surface tension of water," The Journal of Chemical Physics 125, 014702 (2006).

[8] R. Sakamaki, A. K. Sum, T. Narumi, and K. Yasuoka, "Molecular dynamics simulations of vapor/liquid coexistence using the nonpolarizable water models," The Journal of Chemical Physics 134, 124708 (2011).

[9] M. Sega and C. Dellago, "Long-Range Dispersion Effects on the Water/Vapor Interface Simulated Using the Most Common Models," The Journal of Physical Chemistry B 121, 3798–3803 (2017).

[10] O. Wohlfahrt, C. Dellago, and M. Sega, "Ab initio structure and thermodynamics of the rpbe-d3 water/vapor interface by neural-network molecular dynamics," The Journal of Chemical Physics 153, 144710 (2020).

[11] M. J. McGrath, J. I. Siepmann, I.-F. W. Kuo, and C. J. Mundy, "Vapor-liquid equilibria of water from first principles: Comparison of density functionals and basis sets," Molecular Physics 104, 3619–3626 (2006).

[12] M. J. McGrath, J. I. Siepmann, I.-F. W. Kuo, C. J. Mundy, J. VandeVondele, J. Hutter, F. Mohamed, and M. Krack, "Simulating fluid-phase equilibria of water from first principles," The Journal of Physical Chemistry A 110, 640–646 (2006).

[13] M. D. Baer, C. J. Mundy, M. J. McGrath, I.-F. W. Kuo, J. I. Siepmann, and D. J. Tobias, "Re-examining the properties of the aqueous vapor–liquid interface using dispersion corrected density functional theory," The Journal of Chemical Physics 135, 124712 (2011).

[14] C. J. Tainter, L. Shi, and J. L. Skinner, "Reparametrized E3B (Explicit Three-Body) Water Model Using the TIP4P/2005 Model as a Reference," Journal of Chemical Theory and Computation 11, 2268–2277 (2015).

[15] R. Kumar and J. L. Skinner, "Water Simulation Model with Explicit Three-Molecule Interactions," The Journal of Physical Chemistry B 112, 8311–8318 (2008).

[16] H. J. Berendsen, J. R. Grigera, and T. P. Straatsma, "The missing term in effective pair potentials," The Journal of Physical Chemistry 91, 6269–6271 (1987).

[17] W. L. Jorgensen, J. Chandrasekhar, J. D. Madura, R. W. Impey, and M. L. Klein, "Comparison of simple potential functions for simulating liquid water," The Journal of Chemical Physics 79, 926–935 (1983).

[18] H. W. Horn, W. C. Swope, J. W. Pitera, J. D. Madura, T. J. Dick, G. L. Hura, and T. Head-Gordon, "Development of an improved four-site water model for biomolecular simulations: TIP4P-Ew," The Journal of Chemical Physics 120, 9665–9678 (2004).

[19] J. L. Abascal and C. Vega, "A general purpose model for the condensed phases of water: TIP4P/2005," The Journal of Chemical Physics 123 (2005), 10.1063/1.2121687.

[20] P. Paricaud, M. Předota, A. A. Chialvo, and P. T. Cummings, "From dimer to condensed phases at extreme conditions: Accurate predictions of the properties of water by a Gaussian charge polarizable model," The Journal of Chemical Physics 122, 244511 (2005).

[21] O. Lobanova, C. Avendaño, T. Lafitte, E. A. Müller, and G. Jackson, "SAFT-γ force field for the simulation of molecular fluids: 4. A single-site coarse-grained model of water applicable over a wide temperature range," Molecular Physics 113, 1228–1249 (2015).

[22] H. Jiang, O. A. Moultos, I. G. Economou, and A. Z. Panagiotopoulos, "A Hydrogen-Bonding Polarizable Intermolecular Potential Model for Water." The Journal of Physical Chemistry B 120, 12358–12370 (2016).

[23] P. T. Kiss and A. Baranyai, "A systematic development of a polarizable potential of water," The Journal of Chemical Physics 138 (2013), 10.1063/1.4807600.

[24] P. Ren and J. W. Ponder, "Polarizable atomic multipole water model for molecular mechanics simulation," The Journal of Physical Chemistry B 107, 5933–5947 (2003).

[25] J. W. Ponder, C. Wu, P. Ren, V. S. Pande, J. D. Chodera, M. J. Schnieders, I. Haque, D. L. Mobley, D. S. Lambrecht, R. A. DiStasio, M. Head-Gordon, G. N. I. Clark, M. E. Johnson, and T. Head-Gordon, "Current status of the amoeba polarizable force field," The Journal of Physical Chemistry B 114, 2549–2564 (2010), pMID: 20136072.

[26] L.-P. Wang, T. Head-Gordon, J. W. Ponder, P. Ren, J. D. Chodera, P. K. Eastman, T. J. Martinez, and V. S. Pande, "Systematic improvement of a classical molecular model of water," The Journal of Physical Chemistry B 117, 9956–9972 (2013), pMID: 23750713.

[27] M. L. Laury, L. P. Wang, V. S. Pande, T. Head-Gordon, and J. W. Ponder, "Revised Parameters for the AMOEBA Polarizable Atomic Multipole Water Model," The Journal of Physical Chemistry B 119, 9423–9437 (2015).

[28] C. Vega, J. L. Abascal, and I. Nezbeda, "Vapor-liquid equilibria from the triple point up to the critical point for the new generation of TIP4P-like models: TIP4P/Ew, TIP4P/2005, and TIP4P/ice," The Journal of Chemical Physics 125, 034503 (2006).

[29] B. Chen, J. I. Siepmann, and M. L. Klein, "Simulating vapor-liquid nucleation of water: A combined histogram-reweighting and aggregation-volume-bias Monte Carlo investigation for fixed-charge and polarizable models," The Journal of Physical Chemistry A 109, 1137–1145 (2005).

[30] V. Babin, C. Leforestier, and F. Paesani, "Development of a "first principles" water potential with flexible monomers: Dimer potential energy surface, VRT spectrum, and second virial coefficient," Journal of Chemical Theory and Computation 9, 5395–5403 (2013).

[31] V. Babin, G. R. Medders, and F. Paesani, "Development of a "first principles" water potential with flexible monomers. II: Trimer potential energy surface, third virial coefficient, and small clusters," Journal of Chemical Theory and Computation 10, 1599–1607 (2014).

[32] G. R. Medders, V. Babin, and F. Paesani, "Development of a "first-principles" water potential with flexible monomers. III. Liquid phase properties," Journal of Chemical Theory and Computation 10, 2906–2910 (2014).

[33] S. K. Reddy, S. C. Straight, P. Bajaj, C. Huy Pham, M. Riera, D. R. Moberg, M. A. Morales, C. Knight, A. W. Götz, and F. Paesani, "On the accuracy of the MB-pol many-body potential for water: Interaction energies, vibrational frequencies, and classical thermodynamic and dynamical properties from clusters to liquid water and ice," The Journal of Chemical Physics 145, 194504 (2016).

[34] S. K. Reddy, D. R. Moberg, S. C. Straight, and F. Paesani, "Temperature-dependent vibrational spectra and structure of liquid water from classical and quantum simulations with the mb-pol potential energy function," The Journal of Chemical Physics 147, 244504 (2017), https://doi.org/10.1063/1.5006480.

[35] D. R. Moberg, D. Becker, C. W. Dierking, F. Zurheide, B. Bandow, U. Buck, A. Hudait, V. Molinero, F. Paesani, and T. Zeuch, "The end of ice i," Proceedings of the National Academy of Sciences 116, 24413–24419 (2019), https://www.pnas.org/content/116/49/24413.full.pdf.

[36] "Mbx: A many-body energy calculator," http://paesanigroup.ucsd.edu/software/mbx.html, accessed: 2021-02-17.

[37] S. Plimpton, "Fast parallel algorithms for short-range molecular dynamics," Journal of Computational Physics 117, 1–19 (1995).

[38] M. Ceriotti, J. More, and D. E. Manolopoulos, "i-pi: A python interface for ab initio path integral molecular dynamics simulations," Computer Physics Communications 185, 1019–1026 (2014).

[39] P. Eastman, M. S. Friedrichs, J. D. Chodera, R. J. Radmer, C. M. Bruns, J. P. Ku, K. A. Beauchamp, T. J. Lane, L.-P. Wang, D. Shukla, T. Tye, M. Houston, T. Stich, C. Klein, M. R. Shirts, and V. S. Pande, "Openmm 4: A reusable, extensible, hardware independent library for high performance molecular simulation," Journal of Chemical Theory and Computation 9, 461–469 (2013), pMID: 23316124, https://doi.org/10.1021/ct300857j.

[40] Y. Liu, T. Lafitte, A. Z. Panagiotopoulos, and P. G. Debenedetti, "Simulations of vapor–liquid phase equilibrium and interfacial tension in the CO2–H2O–NaCl system," AIChE Journal 59, 3514–3522 (2013).

[41] A. Statt, H. Casademunt, C. P. Brangwynne, and A. Z. Panagiotopoulos, "Model for disordered proteins with strongly sequence-dependent liquid phase behavior," The Journal of Chemical Physics 152, 075101 (2020), https://doi.org/10.1063/1.5141095.

[42] K. S. Silmore, M. P. Howard, and A. Z. Panagiotopoulos, "Vapour–liquid phase equilibrium and surface tension of fully flexible lennard–jones chains," Molecular Physics 115, 320–327 (2017), https://doi.org/10.1080/00268976.2016.1262075.

[43] J. Mayer and M. Goeppert-Mayer, Statistical Mechanics (John Wiley & Sons, New York, 1940).

[44] H. Partridge and D. W. Schwenke, "The determination of an accurate isotope dependent potential energy surface for water from extensive ab initio calculations and experimental data," The Journal of Chemical Physics 106, 4618–4639 (1997).

[45] K. Tang and J. P. Toennies, "An improved simple model for the van der waals potential based on universal damping functions for the dispersion coefficients," The Journal of Chemical Physics 80, 3726–3741 (1984).

[46] C. Burnham, D. Anick, P. Mankoo, and G. Reiter, "The vibrational proton potential in bulk liquid water and ice," The Journal of Chemical Physics 128, 154519 (2008).

[47] B. J. Braams and J. M. Bowman, "Permutationally invariant potential energy surfaces in high dimensionality," International Reviews in Physical Chemistry 28, 577–606 (2009).

[48] H. Kamberaj, R. J. Low, and M. P. Neal, "Time reversible and symplectic integrators for molecular dynamics simulations of rigid molecules," The Journal of Chemical Physics 122, 224114 (2005).

[49] J. Zinn-Justin, "Precise determination of critical exponents and equation of state by field theory methods," Physics Reports 344, 159–178 (2001), renormalization group theory in the new millennium.

[50] P. Linstrom and W. Mallard, NIST Chemistry WebBook, NIST Standard Reference Database Number 69 (National Institute of Standards and Technology, Gaithersburg MD) p. 20899.

[51] K. Binder and M. Müller, "Computer simulation of profiles of interfaces between coexisting phases: Do we understand their finite size effects?" International Journal of Modern Physics C 11, 1093–1113 (2000), https://doi.org/10.1142/S012918310000095X.

[52] F. G. J. Longford, J. W. Essex, C.-K. Skylaris, and J. G. Frey, "Unexpected finite size effects in interfacial systems: Why bigger is not always better—increase in uncertainty of surface tension with bulk phase width," The Journal of Chemical Physics 148, 214704 (2018), https://doi.org/10.1063/1.5025887.

[53] P. K. Yuet and D. Blankschtein, "Molecular dynamics simulation study of water surfaces: Comparison of flexible water models," The Journal of Physical Chemistry B 114, 13786–13795 (2010), pMID: 20939552, https://doi.org/10.1021/jp1067022.

[54] G. Raabe and R. J. Sadus, "Molecular dynamics simulation of the dielectric constant of water: The effect of bond flexibility," The Journal of Chemical Physics 134, 234501 (2011), https://doi.org/10.1063/1.3600337.

IX. GOVERNMENT LICENSE

Supporting information for:
Vapor-liquid equilibrium of water with the MB-pol many-body potential

Maria Carolina Muniz,[1, a)] Thomas E. Gartner III,[2, a)] Marc Riera,[3] Christopher Knight,[4] Shuwen Yue,[1] Francesco Paesani,[3, 5, 6, b)] and Athanassios Z. Panagiotopoulos[1, c)]

[1)] *Department of Chemical and Biological Engineering, Princeton University, Princeton, New Jersey 08544, USA*

[2)] *Department of Chemistry, Princeton University, Princeton, New Jersey 08544, USA*

[3)] *Department of Chemistry and Biochemistry, University of California, San Diego, La Jolla, California 92093, USA*

[4)] *Computational Science Division, Argonne National Laboratory, Argonne, Illinois 60439, USA*

[5)] *Materials Science and Engineering, University of California San Diego, La Jolla, California 92093, USA*

[6)] *San Diego Supercomputer Center, University of California San Diego, La Jolla, California 92093, USA*

(Dated: 15 March 2021)

I. SURFACE TENSION

TABLE I. Surface tension results (N/m). Uncertainties indicate 95% confidence intervals that were obtained from dividing simulations into 10 blocks.

T(K)	Exp[1].	Flexible-512	Rigid-512	Rigid-1024
400	0.054	0.053 ± 0.005	0.053 ± 0.001	0.053 ± 0.002
425	0.048	0.046 ± 0.003	0.047 ± 0.002	0.047 ± 0.002
450	0.043	0.047 ± 0.003	0.041 ± 0.001	0.042 ± 0.003
475	0.037	0.036 ± 0.004	0.035 ± 0.002	0.037 ± 0.003
500	0.031	0.028 ± 0.004	0.032 ± 0.001	0.029 ± 0.001
525	0.026	0.025 ± 0.003	0.025 ± 0.002	0.022 ± 0.002
550	0.020	0.021 ± 0.004	0.020 ± 0.002	0.018 ± 0.002
575	0.014	0.013 ± 0.003	0.015 ± 0.002	0.009 ± 0.003
600	0.008	–	–	0.007 ± 0.002

[a)] These authors contributed equally to this work.

[b)] Electronic mail: fpaesani@ucsd.edu

[c)] Electronic mail: azp@princeton.edu

II. VAPOR PRESSURES

TABLE II. Vapor pressure results (MPa). Uncertainties indicate 95% confidence intervals that were obtained from dividing simulations into 10 blocks.

T(K)	Exp.[1]	Flexible-512	Rigid-512	Rigid-1024
400	0.24577	0.40 ± 0.01	0.298 ± 0.002	0.270 ± 0.001
425	0.50025	0.63 ± 0.03	0.592 ± 0.004	0.524 ± 0.006
450	0.93220	1.19 ± 0.05	1.06 ± 0.01	0.854 ± 0.006
475	1.6160	2.1 ± 0.1	1.72 ± 0.01	1.78 ± 0.02
500	2.6392	2.7 ± 0.1	2.82 ± 0.02	2.99 ± 0.02
525	4.1019	4.6 ± 0.2	5.44 ± 0.05	4.53 ± 0.04
550	6.1172	9.2 ± 0.4	6.91 ± 0.06	7.05 ± 0.06
575	8.8140	9.4 ± 0.4	10.4 ± 0.1	10.7 ± 0.1
600	12.345	–	–	14.5 ± 0.2

III. ENTHALPY OF VAPORIZATION

TABLE III. Enthalpy of vaporization results (KJ/mol). Uncertainties indicate 95% confidence intervals that were obtained from dividing simulations into 10 blocks.

T(K)	Exp.[1]	Flexible-512	Rigid-512	Rigid-1024
400	39.3227	39 ± 1	39.4 ± 0.8	39.8 ± 0.5
425	37.975	37 ± 1	37.8 ± 0.7	38.0 ± 0.7
450	36.486	36 ± 1	36.5 ± 0.5	36.7 ± 0.5
475	34.814	34 ± 1	34.8 ± 0.3	34.9 ± 0.3
500	32.914	32 ± 1	32.6 ± 0.3	32.5 ±0.2
525	30.725	30 ± 1	28.9 ± 0.8	30.0 ± 0.4
550	28.155	25 ± 1	27.1 ± 0.3	26.9 ± 0.3
575	25.052	23 ± 1	23.2 ± 0.3	22.5 ± 0.4
600	21.123	–	–	18.6 ± 0.3

IV. COEXISTENCE DENSITIES

TABLE IV. Liquid and vapor coexistence densities (g/cm^3). Uncertainties indicate 95% confidence intervals that were obtained from dividing simulations into 10 blocks.

T(K)	Phase	Exp[1].	Flexible-512	Rigid-512	Rigid-1024
400	L	0.93749	0.934± 0.001	0.9273± 0.0002	0.9284 ± 0.0006
400	V	0.0013694	0.0019± 0.0006	0.0017± 0.0003	0.0015 ± 0.0002
425	L	0.91527	0.910± 0.001	0.9025± 0.0005	0.9041 ± 0.0005
425	V	0.0026693	0.0029 ± 0.0006	0.0032 ± 0.0004	0.0028 ± 0.0003
450	L	0.89034	0.883± 0.002	0.8761±0.0003	0.8773 ± 0.0006
450	V	0.0048120	0.005± 0.001	0.0055± 0.0005	0.0044 ± 0.0004
475	L	0.86249	0.854± 0.002	0.8463± 0.0006	0.8470 ± 0.0005
475	V	0.0081598	0.0095± 0.0009	0.0086 ± 0.0004	0.0090 ± 0.0004
500	L	0.83131	0.821±0.002	0.8114 ±0.0007	0.8138 ± 0.0009
500	V	0.013199	0.0147±0.0009	0.0141 ±0.0007	0.0152 ± 0.0007
525	L	0.79613	0.783±0.003	0.769 ±0.007	0.775 ± 0.001
525	V	0.020617	0.023± 0.002	0.030 ± 0.006	0.023 ± 0.002
550	L	0.75581	0.73±0.01	0.730 ±0.001	0.731 ± 0.001
550	V	0.031474	0.05± 0.02	0.037 ±0.002	0.0379 ± 0.0021
575	L	0.70830	0.687±0.005	0.677 ±0.003	0.674 ± 0.007
575	V	0.047607	0.057±0.006	0.061 ±0.003	0.065 ± 0.006
600	L	0.64941	–	–	0.61 ± 0.01
600	V	0.072842	–	–	0.095 ± 0.008

V. REFERENCES

[1] P. Linstrom and W. Mallard, *NIST Chemistry WebBook, NIST Standard Reference Database Number 69* (National Institute of Standards and Technology, Gaithersburg MD) p. 20899.